

## Some aspects of electron transfer sensitization systems

Takeo Shimidzu, Tomokazu Iyoda, and Kenichi Honda

Division of Molecular Engineering, Graduate School of Engineering,  
Kyoto University, Sakyo-ku, Kyoto 606, Japan

**Abstract** - Some aspects of electron transfer sensitization systems not only for chemical conversion and storage of light energy but also for design of photoelectrochemical molecular device are presented. Also regarding energy conversion as one of chemical transformation of every chemical signal (information), we have been introducing and realizing the concepts of molecular electronic device. This paper involves 4 subjects for the former and 2 subjects for the latter. (1) Visible-light-induced water reduction with dye-sensitized semiconductor powder catalysts. (2) Regulation of photo-redox cycle of water-soluble metalloporphyrins. (3) Electron transfer of the excited triplet state of water-soluble palladium porphyrins. (4) Photo-induced electron transfer of accordion-type porphyrin cluster. (5) Materialization of photo-active functional molecules with conducting polymer matrices. (6) Multi-mode chemical signal transducer.

### INTRODUCTION

Photochemical reactions have been recognized as peculiarities different from thermal ones. They are induced externally by light irradiation. The resulting excited species should be grasped not to be similar to its ground-state with respect to reactivity and selectivity. Therefore, such photochemical reactions are effective for accumulation of free energy, i.e., (electro)chemical conversion and storage of light energy, and the term of 'photo-induced' is to be applied to photo-chemical signal transducer, i.e., a powerful tool for designing molecular electronic devices. Throughout our recent work, e.g., electron transfer reactions have been also utilized for controlling photochemical signal transducers as well as for designing light-energy conversion systems. Here, we present some aspects of electron transfer sensitization systems, aiming at both. This paper involves 4 subjects for regulating photo-induced electron transfer and 2 subjects for elementary and fundamental technique in order to construct the promising molecular electronic devices, as follows:

- (1) We demonstrated visible-light-induced water reduction with dye-sensitized semiconductor powder catalyst. Its reductive electron transfer mechanism through the excited triplet state of dyes are proposed and then the efficiency and the durability of the system are improved by external heavy atom effect.
- (2) We clarified visible-light-induced redox properties of water-soluble porphyrin gold complexes which have the most anodically-shifted redox potentials. And, a simple photo-redox cycle with no undesired side-reactions is achieved by fixing them in polymer matrices.
- (3) We determined the redox potentials of the excited triplet state of water-soluble porphyrin palladium complexes and presumed one of molecular orientation of the encounter complex in photo-induced electron transfer process.
- (4) We clarified a new class of water-soluble porphyrin aggregates, i.e., accordion-type and side-on-face type aggregates, and investigated photo-induced electron transfer processes of their specific porphyrin aggregates. The charge separation state of side-on-face type ZnTSP-AuTSP aggregate showed much long lifetime up to ms order.
- (5) We demonstrated the preparative methods for materializing photo-active functional molecules with conducting polymer and, in other words, for functionalizing conducting polymer modified electrode/catalyst.
- (6) We realized a new class of concept designing molecular electronic devices, i.e., multi-mode chemical signal transducer.

The above subjects are to be introduced together with their relating recent works.

## 1. VISIBLE-LIGHT-INDUCED WATER REDUCTION WITH DYE-SENSITIZED SEMICONDUCTOR POWDER CATALYST

Significant progress on the photo-induced water reduction to molecular hydrogen has been made by two main approaches. One is a particulate (platinized) semiconductor catalyst (Sc or Sc/Pt) with band-gap excitation, and the other is a homogeneous photoinduced redox system containing a sensitizer, an electron relay, and a micro-dispersed Pt catalyst. However, they have some shortcomings: The former has photoaction with near-UV light and tends to photocorrode, and the latter has no anisotropic reaction fields available for charge separation and unidirectional electron transport. The third approach, the dye sensitization of a particulate Sc or Sc/Pt catalyst, has been proposed in an attempt to combine these two methods. This approach can be applied to various sensitizers and various Sc supports, so that we have dealt with some xanthene dyes (Fig. 1) as sensitizers in order to explore the mechanism and the requirements for working the catalyst.

### 1.1 Visible-light-induced hydrogen production with xanthene dye-Sc/Pt catalyst

Visible light illumination (>420 nm) of xanthene dye (0.4 mM) and triethanolamine (TEA, 0.2 M) in aqueous solution (5ml) particulate Sc/Pt (5 or 10 wt%Pt) resulted in efficient hydrogen production. The xanthene dye bearing more heavy-halogen substituents had larger initial hydrogen production rate ( $r_0$ ). Large differences in catalytic activities are observed among various Sc supports. While uranine-ZnO/Pt catalyst produced hydrogen almost steadily at 0.09 mol/min with no spectral changes, rose bengal-ZnO/Pt catalyst bearing large  $r_0$  (1.23 mol/min) had a break point at 1.5 h of illumination (Fig. 2). The decreased rate (0.08 mol/min), similar to  $r_0$  with uranine-ZnO/Pt catalyst, was sustained for over 10 hr after the break point. By some experimental evidences, it was concluded that rose bengal was photo-dehalogenated, followed by uranine formation. These phenomena were also observed in other heavy-halogenated xanthene dye-sensitized catalysts. Heavy-halogen substituents in xanthene dyes play a significant role in enhancing the intrinsic catalytic activity by the internal heavy-atom effect (internal HAE).

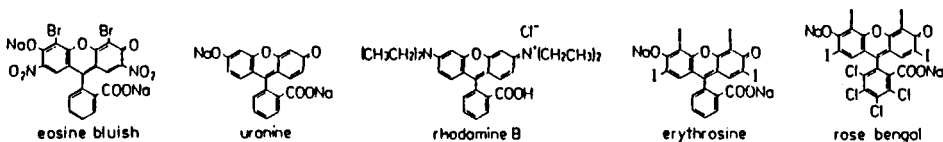


Figure 1. The structures of some xanthene dyes adopted as a sensitizer in the present hydrogen production.

### 1.2 External heavy-atom effect on the present hydrogen production

Based on the above observations, alternatively, we applied the external HAE. The addition of I<sup>-</sup> (0.2 mol/l) in uranine-ZnO/Pt catalyst enhanced the hydrogen production rate by over 11 times, up to 1.04 mol/min (apparent quantum yield > 0.22% at 492 nm). During the photolysis, no decrease of the enhanced  $r_0$  and no photodeterioration were observed. No hydrogen was produced in uranine-ZnO/Pt-I<sup>-</sup> without TEA. After 20 hr the enhanced rate gradually decreased, but the it was restored by the new addition of TEA, not by that of I<sup>-</sup>. These observations suggested that the enhanced catalytic activity of uranine is explained by the external HAE of the added I<sup>-</sup>.

Occurrence of the present external HAE was confirmed by the following evidence. (1) The enhancement by the addition of heavy-atom, I<sup>-</sup>, Br<sup>-</sup>, Cl<sup>-</sup>, Cs<sup>+</sup>, Xe, and so on, was observed. (2) The fluorescence at 520 nm of uranine was efficiently quenched by I<sup>-</sup> and Br<sup>-</sup>, and at 77K a phosphorescence of uranine was emitted at 620 nm in the presence of I<sup>-</sup>. These observations coincided with an increase of real excited triplet quantum yield ( $\Phi_{TM}$ ) of uranine by the external HAE of I<sup>-</sup>. (3) The external HAE was applied to explain the other xanthene dye sensitized catalysts. Uranine and rhodamine B have small  $\Phi_{TM}$  but large  $F(I^-)_{max}$ , while rose bengal and erythrosine have large  $\Phi_{TM}$  with  $F(I^-)_{max}$  of almost unity. The apparent quantum yields enhanced by the external HAE, uranine-ZnO/Pt-I<sup>-</sup> and rhodamine B-ZnO/Pt-I<sup>-</sup>, reached over 0.2 of that of rose bengal-ZnO/Pt catalyst in the first stage. (4) A Wilkinson-type analysis for uranine and rhodamine B with ZnO/Pt was carried out in order to confirm the T<sub>1</sub>-intermediate mechanism was applied to the relationship between fluorescence quenching and enhancement of hydrogen production rate with heavy atom additives. The success of the analysis demonstrated that T<sub>1</sub> states of the chosen dyes are precursors of the electron-injecting species. (5) A new absorption band at 393 nm was observed on illuminating the deaerated aqueous solution containing uranine and TEA without Sc/Pt. This 393 nm absorption band was assigned to uranine anion radical. The long lifetime (42 s) at pH 8 and negative redox potential (-1.36 V vs SCE) enough to reduce a proton imply that the uranine anion radical is the electron-injecting species to Sc/Pt in this hydrogen production.

The reductive electron transfer mechanism through the T<sub>1</sub> state of the dye is proposed (Scheme 1). Heavily-halogenated xanthene dyes have high quantum yields of hydrogen

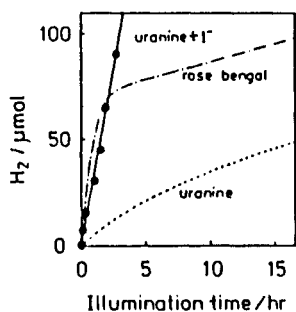
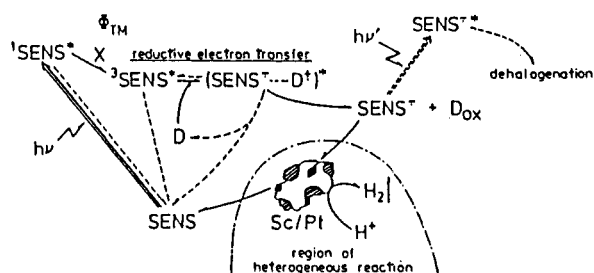


Figure 2. The time courses of the hydrogen production with rose bengal- (---) or uranine- (---) ZnO/Pt-TEA systems and with uranine-ZnO/Pt-TEA-I<sup>-</sup> (●). [dye] =  $4.0 \times 10^{-4}$  mol·L<sup>-1</sup>, [TEA] = 0.2 mol·L<sup>-1</sup>, ZnO/Pt (10 wt % Pt) 6 mg·mL<sup>-1</sup>. The deaerated photolysis solution (5 mL) was illuminated with >420 nm.

### Scheme 1

The Mechanism of the Visible-Light-Induced Water Reduction with the Present Dye-Sensitized Particulate Sc/Pt Catalyst<sup>a</sup>



<sup>a</sup> SENS, D, and X are a dye, an electron donor, and a heavy-atom additive, respectively. Solid lines and broken lines show desired hydrogen-production processes and undesired other processes such as a thermal back-electron transfer process, deactivation one, and a photodehalogenation one.

production but tend to photodehalogenate, while nonhalogenated xanthene dyes have high durability against any photodeterioration but have moderate catalytic activities. The present advanced catalyst, i.e., uranine or rhodamine B - Sc/Pt - I<sup>-</sup> - TEA, has the pronounced advantages of high quantum yield and high durability, which are acquired through the use of durable dyes and the application of the external HAE.

## 2. REGULATION OF PHOTO-REDOX CYCLE OF WATER-SOLUBLE METALLOPORPHYRINS

The design of the photo-chemical energy conversion system using a metalloporphyrin as a visible-light sensitizer involves some photoelectrochemically fundamental interests in connection with the primary photochemical processes in natural photosynthesis. Compared with appreciable successes in photo-reduction of water, some problems have still remained in the photo-oxidation of water: (1) thermodynamic requirements enough to photo-oxidize water and (2) undesired irreversible reactions of the oxidized porphyrin. A metalloporphyrin having high oxidizing power is obtained by the incorporation with an electronegative central metal such as gold (EN=2.54). Also, it is necessary to design a simple redox cycle without undesired reactions. AuTMPyP (TMPyP=tetra(4-N-methylpyridyl)porphyrin) is suitable as a photosensitizer through reductive electron transfer cycle (RET) (cf. oxidative electron transfer=OET).

### 2.1 Redox processes of water-soluble porphyrin gold complexes in homogeneous solution

Photo-oxidized product of AuTMPyP with K<sub>2</sub>S<sub>2</sub>O<sub>8</sub>, sacrificial oxidant was 'hydroxyporphyrin'. The products were bleached upon further irradiation and was not reduced back with electron donor at all. Similar to the case of other metalloporphyrins, the formation of the 'hydroxyporphyrin' through the OET process became a fatal obstacle toward photo-redox cycle. On the other hand, AuTMPyP was photo-reduced with various sacrificial electron donors (e.g. ethylenediaminetetraacetic acid (EDTA) and its metal complexes (Mg-EDTA, Ni-EDTA) and TEA). In all cases, the product was AuTMPyP phlorin at pH<9 or AuTMPyP π-radical anion at pH=10 (Fig. 3). The AuTMPyP π-radical anion was completely oxidized back to the parent AuTMPyP with O<sub>2</sub> or K<sub>2</sub>S<sub>2</sub>O<sub>8</sub> at pH>9. The AuTMPyP phlorin was oxidized back to the parent AuTMPyP with K<sub>2</sub>S<sub>2</sub>O<sub>8</sub> at pH 1-8.

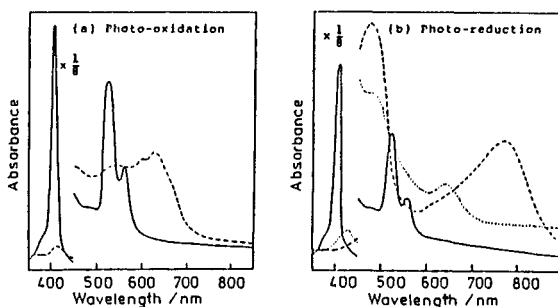
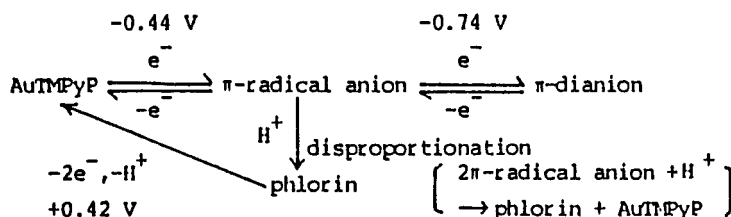


Figure 3 -The absorption spectra of photo-oxidized AuTMPyP with K<sub>2</sub>S<sub>2</sub>O<sub>8</sub> (a) and photo-reduced AuTMPyP with EDTA (b). (a) —, AuTMPyP ; ---, isoporphyrin and its rearranged products. (b) —, AuTMPyP ; ---, π-radical anion; ----, phlorin (AuTMPyPH<sup>-</sup>).

From flash photolysis studies of AuTMPyP with EDTA at pH 4.8, the absorbance decay assigned to photogenerated  $\pi$ -radical anion followed by second-order kinetics with the rate constant of  $2.6 \times 10^4 \text{ M}^{-1} \text{ S}^{-1}$ , and in turn AuTMPyP phlorin increased. The disproportionation of the AuTMPyP  $\pi$ -radical anion was also confirmed by addition of HCl to the photo-generated  $\pi$ -radical anion solution. Rotating ring-disk voltammograms (Fig. 4) were obtained in AuTMPyP containing  $\text{Na}_2\text{SO}_4$ . At pH=10 the cathodic disk limiting current ( $I_D$ ) was observed in two steps corresponding to the first and the second reductions of AuTMPyP. In the first reduction region, anodic ring current ( $I_R$ ) corresponding to re-oxidation of the  $\pi$ -radical anion was observed at  $E_R > -0.46 \text{ V}$  ( $E_R$ : ring potential). In the second reduction region, however, no ring current was observed. These observations indicated that the  $\pi$ -dianion of AuTMPyP was not stable and not converted to phlorin at pH=10. At the lower pH ( $3 < \text{pH} < 6$ ), the collection efficiency (at  $E_R < 0.36 \text{ V}$ ) of the AuTMPyP  $\pi$ -radical anion is smaller than that at pH=10 (85-90%). It is indicated that the AuTMPyP  $\pi$ -radical anion is converted to the AuTMPyP phlorin at a low pH. Consequently, these observations suggested that the AuTMPyP phlorin was generated via only disproportionation of the  $\pi$ -radical anion.

The present RET process of AuTMPyP provides an durable photo-catalytic reaction and its energetics are summarized in Scheme 2. At pH<3.5, hydrogen was produced in the presence of AuTMPyP, colloidal Pt catalyst and EDTA under visible-light irradiation.

Scheme 2



The mechanism of reductive electron transfer of AuTMPyP

## 2.2 Regulation of photo-redox processes of the gold porphyrins in polymer matrix

Since the disproportionation reaction is bimolecular reaction of the  $\pi$ -radicals, it is expected that the disproportionation is inhibited by electrostatic fixation on polyelectrolytes such as Nafion. The AuTMPyP was fixed on Nafion using two methods. For the photo-redox reaction, a mixture of an aqueous solution of AuTMPyP and an equivalent weight solution of Nafion was mixed with stirring for an hour. For the electrolysis, an indium tin oxide electrode (ITO) spin-coated with Nafion 117 was used. The fixation was performed by dipping the electrode into AuTMPyP aqueous solution. In the presence of Nafion, a considerable stabilization of  $\pi$ -radical anion was observed under visible light illumination. The spectral changes upon steady state irradiation exhibit good isosbestic points, thus indicating clean reduction without successive reaction. When the ionic strength of the bulk increased by the addition of neutral salt, the AuTMPyP was excluded from the Nafion matrix so that it was immediately converted to phlorin in the bulk solution.

Apparent diffusion constant of AuTMPyP fixed on Nafion was measured by chrono-absorptmetry using this modified electrode. The obtained apparent diffusion constant of  $2.3 \times 10^{-13} \text{ cm}^2 \text{ s}^{-1}$  is fairly small compared with diffusion constant of  $1.6 \times 10^{-5} \text{ cm}^2 \text{ s}^{-1}$  obtained by rotating disk electrode experiment in Nafion-free aqueous solution. Thus, it was clear that the mobility of porphyrin was decreased by fixation on Nafion.

## 3. ELECTRON TRANSFER OF EXCITED TRIPLET STATE OF WATER-SOLUBLE Pd PORPHYRINS

The theories on photo-induced electron transfer (ET) were based on several assumptions such as reactant having small spherical structure, solvent being as dielectric continuum, little consideration on molecular geometry and spin states, and so on. In order to reinforce the established theories and also to build up new ones, one deliberately applies the conventional theories to special cases broken away from the above assumptions and still must grasp respectable specificity of the phenomena. Our first subject on the specificity is photo-induced ET of a non-spherical molecule, i.e., metalloporphyrins.

Metalloporphyrins have been widely investigated as a model compound of a reaction center in natural photosynthesis and as an artificial sensitizer for solar energy conversion systems. Relating to water photo-splitting into its elements, water-soluble metalloporphyrins suitable for redox reactions in aqueous solution play a significant role as a sensitizer, ranking with Ru polypyridine complexes. However, there has been few reports on their redox properties in the excited state and still less on nature of photo-induced ET

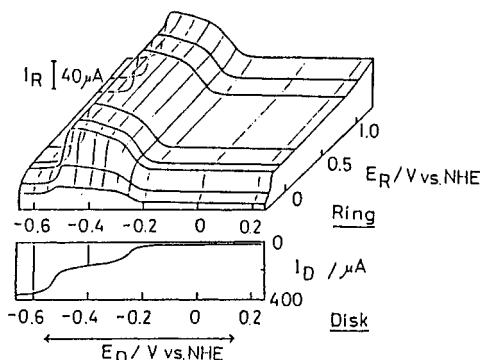


Figure 4 The correlation of RRDE current-potential curves for reduction of AuTMPyP at pH 10.5.  $I_D$ : disk current,  $I_R$ : ring current,  $E_D$ : disk potential,  $E_R$ : ring potential.

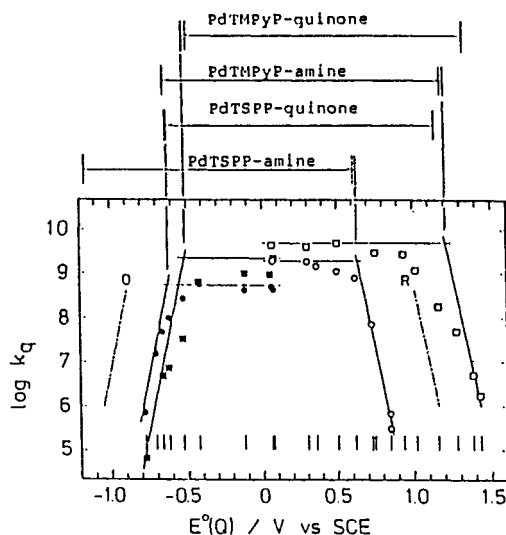


Fig. 5 The correlation between  $\log k_q$  and  $E^o(Q)$ . (—): observed  $*E^o$ , (----): estimated  $*E^o$ , (.....): ground-state  $E^o$

processes because of their complicated transient absorption spectra for monitoring deactivation processes and difficulty of measuring their redox potentials in the ground state. Their Pd, Rh, Ru, and Pt complexes have intense and long-lived phosphorescences at room temperature owing to internal heavy atom effect. Especially, the Pd complexes are easily prepared and have no axial ligands whose role in ET is significant but hard to make clear. Firstly, their excited-triplet-state ( $T_1$ ) redox potential was determined by ET-type phosphorescence quenching with a series of quenchers having various redox potentials.

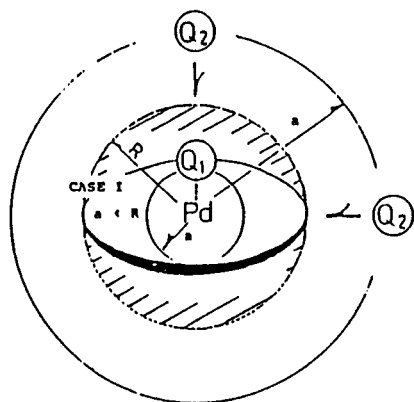
Secondly, applying the energy gap law to the ET processes, significant kinetic parameters, i.e., intrinsic barrier, adiabaticity, and encounter distance, were evaluated by computer simulation technique. We suggested molecular geometry of the encounter complex (EC) by comparing the size of the EC with that of the non-spherical porphyrin. In another sense, the present study appreciated a simple phosphorescence quenching method as a powerful tool for analyzing the ET.

### 3.1 Determination of redox potentials in the excited triplet state

The excited-state redox potential ( $*E(0)$ ) can be estimated by redox potential in the ground state and excitation energy. The present phosphorescence quenching was verified by dynamic ET transfer mechanism. Fig. 5 shows the  $\log k_q$  vs  $E^o(A/A^-)$  or  $E^o(D^+/D)$  (represented as  $E^o(Q)$ ) plots for oxidative and reductive ET's, respectively. The  $\log k_q - E^o(Q)$  plots reflected in relative energetics between the  $*E(0)$  of the  $T_1$  porphyrins and the  $E^o(Q)$ . In sufficiently exoergonic region (downhill ET),  $k_q$ 's were kept constant, which suggested to be diffusion-controlled region. The observed  $k_q$  less than the diffusion-controlled rate ( $7.688 \times 10^9 \text{ sec}^{-1}$ ) indicated some non-adiabaticity of the ET as is described in the later part. Conversely,  $k_q$ 's depended largely on the  $E^o(Q)$  in endoergonic region (uphill ET) which satisfied Arrhenius-type linear relationship with a slope of  $-(1/2.303RT)$  ( $= -16.9 \text{ V}^{-1}$  at 20 C). The  $*E(1)$  was determined according to the method by Meyer et al.  $*E(1)$  is isoenergetic to  $E^o(Q)$  given at an intersecting point of the prolongations between the Arrhenius-type linear portion and the plateau one of diffusion-controlled region. It became clear that the estimation held true also in the water-soluble metallo-porphyrins.

The straightforward approach considering large planer structure of the porphyrin seems to be unique and sound for the analysis of the present specific ET, opposing to the current studies under the assumption of all the species being spherical structure. Additionally, the detailed analysis of the simulation offers a size of the EC and allows us to find a certain molecular geometry of the EC. That is to say, when a quencher approaches to a porphyrin in the axial direction, the quencher recognizes it as a small partner. Conversely in case of the approach in the planer direction, the quencher realizes as a large one. In the present study, whether the ET distance is larger or smaller than the radius of the porphyrin plane is the significant boundary condition so as to visualize the molecular geometry of the EC.

Scheme 3



The molecular orientation of the encounter complex of Pd porphyrin and quencher.

### 3.2 Molecular orientation of the encounter complex

Fig. 6 shows the  $\log k_q - \Delta G$  plots obtained by normalization of Fig. 5. In the present range of  $\Delta G$ , the Agmon-Levine's FER is practically equivalent to FER's by Marcus and Rehm-Weller. The  $\log k_q - \Delta G$  plots were simulated. Under the additional boundary condition that the (PRE W) values at  $\Delta G \ll 0$  are 2.36, 0.68, 15.88, and 2.77 for PdTMPyP-quinone, PdTMPyP-amine, PdTPPS<sub>4</sub>-quinone, and PdTPPS<sub>4</sub>-amine, respectively, the best-fitting curves was obtained. From the values of PRE and W giving the curves, we obtained the intrinsic barrier ( $\Delta G^\ddagger(0)$ ), the electronic transmission coefficient ( $\kappa$ ), and the dissociation rate constant of the EC ( $k_{21}$ ).

All the ET processes had  $< 8$  kJ/mol of intrinsic barrier ( $\Delta G^\ddagger(0)$ ). Except for PdTPPS<sub>4</sub>-quinone, the other systems had small  $\kappa$  values, which suggested non-adiabaticity, i.e., the activation free energy term was dominant in the denominator. The non-adiabaticity and the small intrinsic barrier suggested very weak interaction between the EC and the SIP states.

The ratio of the diffusion rate constant ( $k_{12}$ ) to the dissociation rate constant ( $k_{21}$ ) of the EC has a dimension of concentration and then one can lead the ratio into a size ( $a$ -value) of a certain space which the EC occupies.

$$a = \left[ \frac{3k_{12}}{4\pi N_A k_{21}} \right]^{\frac{1}{3}}$$

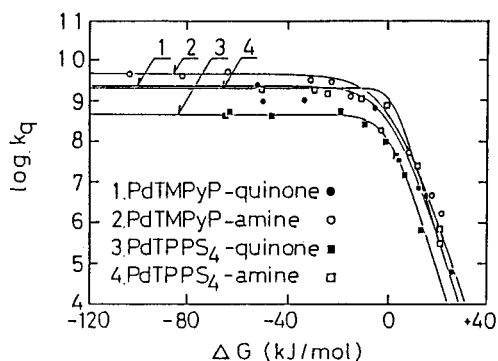
where  $N_A$  is Avogadro's number.

Since the  $a$ -value is the maximum of the EC size calculated under condition that space equally allots a share to each EC, it is not necessarily in agreement with a real size of the EC. However, the axial direction when the quencher approaches to the porphyrin ring is strongly suggested if the  $a$ -value is distinctly smaller than the radius of the porphyrin ring ( $R=10-14$  Å) (Case I). This judgement is significant in the present study. However, if  $a > R$  (case II), we cannot determine the EC structure, i.e., whether the quencher approaches to the porphyrin in the axial or planar direction. Scheme 3 shows the schematic illustration under the above consideration.

## 4. PHOTO-INDUCED ELECTRON TRANSFER OF ACCORDION-TYPE PORPHYRIN CLUSTER

The study on the photoinduced electron transfer reactions using metalloporphyrins as a sensitizer is important for photo-energy conversion into chemical energy. In particular, the study on the role of porphyrin aggregate in charge separation process are noted in connection with the primary process in natural photosynthesis. Both photo-induced charge separations in accordion-type cluster and in side-on-face-type aggregate were studied.

The electron transfer in M<sub>1</sub>TSP-P-M<sub>2</sub>TMPyP cluster was investigated. In the system consisting of AuTSP-P-AuTMPyP accordion-type cluster as an electron acceptor and monomeric ZnTPP as a sensitizer, which has no electrostatic interaction with the cluster, the singlet excited state of ZnTPP was not quenched by AuTSP-P-AuTMPyP cluster but the triplet excited state of ZnTPP was strongly quenched by the cluster. After this quenching, radical anion of Au porphyrins and radical cation of ZnTPP were observed. The result shows that the charge separation was achieved by the oxidative electron transfer process from the triplet excited state of ZnTPP. Similar charge separation between accordion-type cluster and monomeric porphyrins, e.g., Cu, Ag, Pd, and free base porphyrins, were also observed.



$$\Delta G^\ddagger = \Delta G + \frac{\Delta G^\ddagger(0)}{\ln 2} \ln \left[ 1 + \exp \left( - \frac{\Delta G \ln 2}{\Delta G^\ddagger(0)} \right) \right]$$

Figure 6 The correlation between  $\log k_q$  and free energy change obtained by normalization of Fig. 5.

Of the side-on-face-type aggregate consisting of AuTSPP and ZnTSPP, the triplet excited state of ZnTSPP was quenched by AuTSPP, followed by anomalous long-lived charge separation; up to ms order in the aggregate

Also, the accordion-type porphyrin cluster has peculiar internal electron transfer behavior depending on a set of central metals.

## 5. MATERIALIZATION OF PHOTO-ACTIVE FUNCTIONAL MOLECULES WITH CONDUCTING POLYMER MATRICES

On this subject, we present a photochemical-relating part of our recent work on functionalizing and hybridizing conducting polymer matrices with various functional materials. In addition, studies on anisotropic conducting polymer LB film and photo-patterning of conducting polymer onto each materials have been carried out from view point of structural functionalization.

A chemically-modified electrode exhibiting widely specific functions has been developing an active field of electrochemistry and membrane chemistry. Our recent aim has been directed to functionalization of a conducting polymer electrode/catalyst, which is potentially endowed for new performances responsible for its high conducting matrix. We have already established the hybridization procedure of a conducting polypyrrole (PPy) with a negatively-charged functional molecule through anodic doping process on electropolymerization of pyrrole. For example, a charge-controllable membrane, an electrochromic display device, a highly-dispersed metal, nucleic acid sensors, and so on have been demonstrated. Here, applying our procedure to photo-active functional molecules, we constructed dye-incorporated PPy modified electrode and prepared dye-incorporated PPy semiconductor catalyst by photoelectrochemical modification.

### 5.1 Dye-incorporated PPy modified electrode

A negatively-charged dye, e.g., zinc tetra(4-sulfophenyl)porphyrin (ZnTSPP), ruthenium tris(bathophenanthroline-disulfonate), and indigo carmine, was efficiently incorporated in PPy matrix when pyrrole was electropolymerized together with the dye in water or DMF. The incorporation was driven by electrostatic attraction between partially oxidized (doped) PPy chain and negative charges on the dye. The incorporated dye was scarcely released (i.e., undoped) even by electrochemically reducing the PPy matrix, which satisfied our aim to fix the dye in PPy matrix. The resulting PPy showed the same high conductivity as native PPy, so that the amount of the incorporated dye can be controlled electrochemically.

The resulting dye-incorporated PPy modified ITO electrode showed anodic photocurrent ( $>600$  nA/cm<sup>2</sup>) in Fe(CN)<sub>6</sub><sup>3-/4-</sup> containing aqueous solution under  $>690$  nm irradiation. At  $>0.3$  V vs SCE an appreciable anodic photocurrent was build up and its action spectrum agreed with visible absorption spectrum of the incorporated dye. Then, the incorporated dye played a role as a sensitizer through oxidative electron transfer to the ITO electrode. The current quantum efficiency reached ca. 0.1 %. It was demonstrated that this preparative method was worth while endowing PPy with photoresponsive properties.

### 5.2 Photoelectrochemical modification of particulate semiconductor surface with a sensitizer

Some particulate semiconductors catalyze photo-oxidative polymerization of pyrrole in the presence of an appropriate electron acceptor under their band-gap excitation, followed by PPy is adhered on the semiconductor surface. In the presence of Ag<sup>+</sup> and tetra(4-sulfophenyl)porphyrin (TSPP), pyrrole was polymerized into PPy by photo-catalytic action of particulate TiO<sub>2</sub> under  $>300$  nm irradiation and the resulting PPy was deposited on the TiO<sub>2</sub> surface, effectively incorporating TSPP. Visible absorption spectra of the modified TiO<sub>2</sub> suspended solution indicated that TSPP was fixed into PPy matrix on the surface of TiO<sub>2</sub>. This procedure has potential capacity to become a new photoelectrochemical surface modification of a semiconductor catalyst/electrode.

### 5.3 Photo-patterning and anisotropic LB film of conducting polymers

Fabrication of conducting polymer pattern is considered to be one of the most important subject in the field of molecular electronic devices. A novel photo-sensitized polymerization of pyrrole is investigated in order to form fine conducting polymer pattern on insulating materials. In this method, both photosensitizer bearing oxidizing power of pyrrole and sacrificial oxidant which does not directly oxidize pyrrole are required for oxidation of pyrrole. It was proved that the photo-sensitized polymerization proceeded according to the oxidation of pyrrole by photo-oxidized sensitizer through the oxidative electron transfer process. The fine conducting pattern about 10 micrometer width of PPy was formed on organic membrane such as Nafion which adsorbed cationic sensitizer by this method.

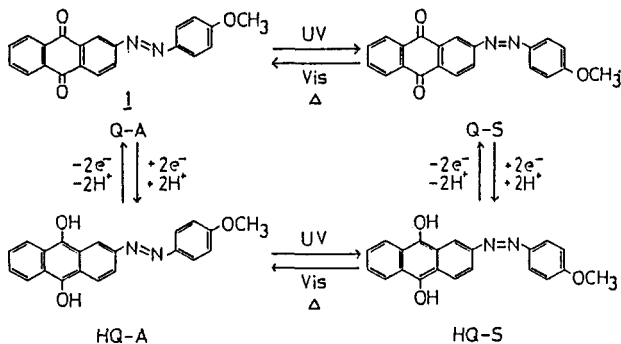
Structural functionalization of conducting polymer is an important problem. Conducting polymer LB film prepared by LB technique and unique electropolymerization showed large anisotropy of conductivity ( $10^{-1}$  S cm<sup>-1</sup> to lateral direction and  $10^{-11}$  S cm<sup>-1</sup> to perpendicular one).

## 6. MULTI-MODE CHEMICAL TRANSDUCER

Since F. L. Carter advocated the concept of a "molecular electronic device", various advanced approaches, both theoretical and experimental, to the promising device have started to take shape with wide interests in science and technology. In order to design a molecule for the coming chemical transducer, one will be forced not only to improve the intrinsic functions but also to endow highly-integrated transformation modes to one molecule. As to one of the latter approaches, we are demonstrating a new class of chemical transducer, which has plural transformation modes by independent stimulations and whose response by one stimulation can be regulated by the other stimulations. The basic requirements are as follows. (1) The molecule has plural regions, i.e., functional groups, responsive independently to stimulations. (2) These regions have appropriate interactions between them, e.g., through conjugated system. So, a molecule with  $n$  responsive regions would have  $2^n$  states corresponding to  $n$  transformation processes by every independent stimulation. Also, all the transformation modes would be dependent each other: one signal transformation process would be, more or less, affected by the states of the other  $n-1$  regions. Such interdependent signal transformation is termed as conjugated functions.

Based on the above concept, we investigated the conjugated transformation of a multi-mode chemical transducer having an electrochromic quinone region and a photochromic azo region in conjugated system, such as 2-(4'-methoxyphenylazo)anthraquinone **1**.

**1** showed both electrochromism due to its quinone-hydroquinone region and photochromism due to its azo region, as one expected. These observations illustrated that **1** had 4 ( $=2^2$ ) distinguishable states corresponding to both redox states of the quinone-hydroquinone region and geometric isomers of the azo region. **1** played a significant role as a new chemical transducer in dual modes, electrochromism and photochromism. Interestingly, both electrochromism and photochromism were expected to be affected one another since the quinone-region was linked to the azo-region through conjugated system. In the thermal isomerization from *syn*- to *anti*-forms, an interdependent transformations were distinctly observed. The *syn*- $\rightarrow$ *anti* thermal isomerization rate of quinone-type was 30 times faster than that of hydroquinone-type, i.e., the isomerization of the azo region was affected by redox states of the quinone region. This conjugated function, characteristic of the present multi-mode chemical transducer, may be applicable for dual-mode memory: One is "shallow" memory mode in quinone-type photochromism easy to be transformed, and the other is "deep" memory mode in hydroquinone-type one hard to be transformed. The present concept will have potential extensions to other responsive functions and provide one of the basic strategies approaching to the promising molecular device. The design of the multiple and interdependent chemical transducer is taking a step forward to equip a molecule with logic functions.



## REFERENCES

Reference numbers correspond to the 6 subjects covered in the manuscript

- (1) T. Shimidzu, T. Iyoda, Y. Koide and N. Kanda, *Nouv. J. Chim.*, 1983 **7** 21-27 and T. Shimidzu, T. Iyoda and Y. Koide, *J. Amer. Chem. Soc.*, 1985, **107**, 35-41.
- (2) K. Yamaguti and S. Sato, *Nouv. J. Chim.* 1986, **10**, 217-221, T. Shimidzu, H. Segawa, T. Iyoda and K. Honda, *J. Chem. Soc., Faraday Trans. 2* 1987, **83**, 2191-2200, and *J. Macromol. Sci. Chem.*, in press.
- (3) To be submitted.
- (4) T. Shimidzu and T. Iyoda, *Chem. Lett.*, 1981, 853-856 and to be submitted.
- (5) T. Iyoda, A. Ohtani, T. Shimidzu and K. Honda, *Chem. Lett.*, 1986, 687-690, T. Shimidzu, A. Ohtani, T. Iyoda, and K. Honda, *J. Chem. Soc., Chem. Commun.*, 1986, 1415, T. Iyoda, M. Ando, T. Kaneko, A. Ohtani, T. Shimidzu and K. Honda, *Tetrahedron Lett.*, 1986, **27**, 5633-5636, *Synth. Metal*, 1987, **18**, 725-730, *ibid.*, 1987, **18**, 745-751, T. Shimidzu, A. Ohtani, T. Iyoda and K. Honda, *J. Chem. Soc., Chem. Commun.*, 1987, 327-328, *Recent Adv. in Electroorg. Synth.*, 1987, 369-372, T. Shimidzu, A. Ohtani, T. Iyoda and K. Honda, *J. Electroanal. Chem.* 1987, **224**, 123-135, and T. Iyoda, M. Ando, T. Kaneko, A. Ohtani, T. Shimidzu and K. Honda, *Langmuir*, 1987, **3**, 1169-1170.
- (6) To be submitted.